

Thermal decomposition study of antimony (III) tribromide and aromatic amine adducts

E. P. S. Martins · J. R. Botelho · S. F. Oliveira ·
L. N. H. Arakaki · M. G. Fonseca · J. G. P. Espínola

Received: 25 September 2008 / Accepted: 20 February 2009 / Published online: 10 June 2009
© Akadémiai Kiadó, Budapest, Hungary 2009

Abstract Solid adducts, $\text{SbBr}_3 \cdot \text{L}$ ($\text{L} =$ pyridine, 2-, 3- and 4-methylpyridine; abbreviated as Py, 2MPy, 3MPy and 4MPy) were synthesized and characterized by elemental analysis and IR spectroscopy. According to the results coordination of nitrogen of aromatic ring with antimony atom was supposed. Kinetic studies were accomplished by using thermogravimetric data obtained through non-isothermal technique. Determination of activation energy and pre-exponential factor was based on the Coats–Redfern integral Ozawa–Flynn–Wall model-free methods. The kinetics parameters E_a , and $\log A$ determined at 5 K min^{-1} were $150.6 \text{ kJ mol}^{-1}$, 16.0 and $122.0 \text{ kJ mol}^{-1}$, 12.4 for $\text{SbBr}_3 \cdot \text{Py}$ and $\text{SbBr}_3 \cdot 4\text{MPy}$, respectively.

Keywords Adduct · Pyridine · Kinetic decomposition

Introduction

Several investigations involving 2-, 3-, and 4-methylpyridine as ligand for transition metal salts have been reported [1–5]. These studies mainly focused on synthetic and structural features of adducts and their thermal decomposition. Especially adducts of elements of the group 15 were reported [6–12]. Some studies explored synthetic procedure and structural characterizations [6]. The reactivity of bases in reaction of ammoxidation over modified SAPO with antimony [7] and power consumption for zinc

electrowinning from acidic sulfate electrolyte [8, 9] were investigated. Chemical energetic variations in formation and decomposition of adducts were determined [10–12]. Between the elements of the group 15, arsenium and antimony are the most studied ones. The preparation, characterization and the kinetic study of adducts of antimony (III) halides (chloride and iodide) with 2-, 3- and 4-methylpyridine was related [12]. In this investigation, thermoanalytical technique was used in determining kinetics parameters as activation energy and pre-exponential factor and, a mechanism possible for decomposition of adducts was suggested.

In the present paper the synthesis and characterization of adducts of antimony (III) tribromide with pyridine and its methyl derivatives are described. Activation energy and the pre-exponential factor of adducts decomposition are estimated by using different methodologies.

Experimental

Chemicals

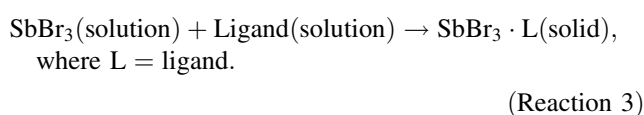
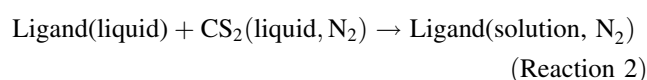
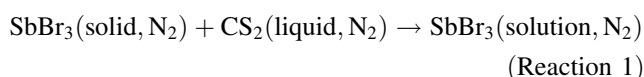
The solvents used in all the preparations were distilled and stored over Linde 4 Å molecular sieve. Pyridine, 2-, 3- and 4-methylpyridine (Merck) were used without further purification. The antimony (III) tribromide salt (Merck) was sublimed and stored under vacuum. All manipulations of antimony (III) tribromide salt were performed under dry conditions in a nitrogen dry-box glove.

Preparations

Four antimony tribromide compounds with pyridine, 2-, 3- and 4-methylpyridine ligands were synthesized by

E. P. S. Martins · J. R. Botelho · S. F. Oliveira ·
L. N. H. Arakaki · M. G. Fonseca (✉) · J. G. P. Espínola
Departamento de Química, CCEN, Universidade Federal da
Paraíba, Caixa Postal 5093, João Pessoa, PB 58059-900, Brazil
e-mail: mgardennia@quimica.ufpb.br

precipitation method from carbon sulfide solutions. In a typical procedure (Reactions 1-3), the carbon sulfide solution of antimony (III) tribromide (2 mmol antimony tribromide dissolved in 50.0 cm³ of solvent) was added to the carbon sulfide solution of the base (2 mmol of each ligand). The obtained mixture was stirred magnetically at room temperature for 2 h under nitrogen atmosphere. After stopping the process of mixing some minutes later a solid was obtained. The precipitate was filtered washed with the same solvent and dried under vacuum. The yields for all adducts preparations were in 85–90%.



Physical measurements

The melting points of all the compounds were determined using Microquímica model MQAPP-301 apparatus. The infrared spectra in the 4,000–400 cm⁻¹ range were obtained with a Bomen model MB-102 spectrophotometer in KBr pellets at room temperature. Carbon, nitrogen and hydrogen contents were determined using a PerkinElmer PE-2400 microelemental analyzer. Antimony content was estimated by atomic absorption using a GBC model 908 AA spectroscopy apparatus after dissolution of each adduct in HNO₃. Bromide content was calculated by using Volhard's method after solving of each adduct in HNO₃. Thermal decomposition was performed by using a Shimadzu TG-50 thermobalance. TG curves were obtained through non-isothermal technique where 5.0 ± 0.5 mg samples were heated under a nitrogen flow rate of 50 cm³ s⁻¹ at 5, 10 and 15 K min⁻¹. The thermogravimetric data were fitting to Ozawa–Flynn–Wall equation [13, 14],

$$\log \beta = \log(AE_a/g(\alpha)R) - 2.315 - 0.457(E_a/RT) \quad (1)$$

where A is the pre-exponential factor, E_a is the activation energy, T is absolute temperature, R is the gas constant, and g(α) is the reaction model. This procedure allowed to calculate the activation energies for the every experimental points of fractional conversion (in the 0.15 < α < 0.95 interval, conjointly from several curves). The same experimental data were used further for searching the topochemical equation (the selection from 12 equations: chemical reactions on the interface, nucleation and

diffusion). In this case the Coats–Redfern equation and the model-fitting method were used:

$$\text{Ln}(g(\alpha)/T^2) = \text{Ln}(AR/\beta E_a [1 - (2RT_{\text{exp}}/E_a)]) - E_a/RT \quad (2)$$

where T_{exp} is the mean experimental temperature.

Kinetic of thermal adducts decomposition

Thermogravimetric data for linear heating at different temperatures were processed according to the model free method without the information about kinetic topochemical equations. ‘Ozawa–Flynn–Wall Analysis’ program [13–17] was used to calculate the dependence of lnβ versus 1/T. It allows to calculate the activation energies for all experimental point of fractional conversion (in the interval 0.02 < α < 0.98, conjointly from several curves). The same set of experimental data was used further for searching the topochemical equation (the selection from 18 equations: chemical reaction on the interface, nucleation, and diffusion [18]). This calculation was made by integral method of Coats–Redfern of simple linear regression [19] for regions of the TG curves where the ‘Model-free’ module program method detected constancy in the kinetic parameter values. If the calculations resulted two or three kinetics equations and same correlation coefficients but with noticeably differences in the kinetics parameters it was reasonable to select an equation with parameter values nearest to one resulted from ‘Model-free’ module program.

Results and discussion

Elemental analysis and infrared spectroscopy

Adducts of SbBr₃ with pyridine and 2-, 3- or 4-methylpyridine ligands were synthesized and characterized by using spectroscopic methods. Results of the elemental analysis results of the solid adducts are in complete agreement with the SbBr₃ · L (L = ligand) general formula as can be seen in Table 1.

The infrared spectra assignments were based on previous reports [20, 21] and the main vibrational absorption bands for adducts and ligands are listed in Table 2. It was observed that some ligand bands in adducts are shifted comparing to the absorptions for free ligand. However, the main vibration bands for adducts showed the same characteristics like the free ligands, suggesting that their vibration modes were not modified after coordination with antimony.

Table 1 Experimental (theoretical) analytical data, melting point (MP) and temperature range of decomposition (ΔT) for adducts of antimony tribromide with pyridine, 2-, 3- and 4-methylpyridines

Adduct	%C	%H	%N	%Br	%Sb	MP (K)	ΔT (K)
SbBr ₃ · Py	13.66 (13.64)	1.15 (1.14)	3.21 (3.18)	54.47 (54.54)	27.35 (27.50)	–	401–494
SbBr ₃ · 2MPy	15.90 (15.86)	1.52 (1.54)	3.11 (3.08)	52.81 (52.86)	26.30 (26.59)	417	401–503
SbBr ₃ · 3MPy	15.80 (15.86)	1.57 (1.54)	3.02 (3.08)	52.87 (52.86)	26.35 (26.59)	421	406–518
SbBr ₃ · 4MPy	15.80 (15.86)	1.55 (1.54)	3.05 (3.08)	52.91 (52.86)	26.49 (26.59)	–	410–513

Table 2 Main absorptions (cm⁻¹) in infrared spectra for adducts and free ligands

Compound	ν_{CC}	$\nu_{CC,CN}$	$\nu_{CC,CN}$	X-sens	δ_{CH}	δ_{CH}	ϕ_{CH}
Py	1586s	1448s	1431s	–	1217w	1146w	718s
SbBr ₃ · Py	1530s	1481s	No	–	1235w	1161w	736s
2MPy	1594s	1478s	1377w	1237w	1295m	1150w	730m
SbBr ₃ · 2MPy	1605s	1471m	1376m	1227w	1278m	1168w	671s
3MPy	1579s	1479s	1414m	1229w	1190m	1126m	711m
SbBr ₃ · 3MPy	1546s	1465m	No	1256m	1183m	No	680s
4MPy	1608s	1490m	1418m	1213w	1286m	1123w	727m
SbBr ₃ · 4MPy	1610s	1469m	1385m	1228m	1280m	1162w	700w

ν stretch; δ bending in-plane; ϕ ring bending out-of-plane; X-sens C–CH₃; s strong band; m medium band and w weak band

Thermogravimetry, DSC and decomposition kinetics

Thermogravimetric curves for all adducts in the 298–823 K temperature range are in Fig. 1, showing a single step thermal decomposition (as resumed in Table 3 and illustrated in Fig. 2).

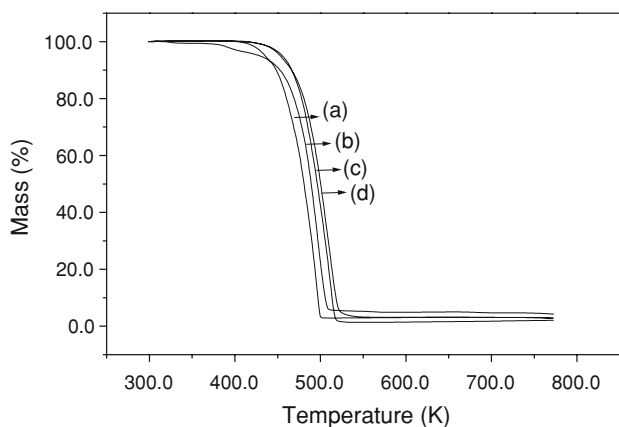
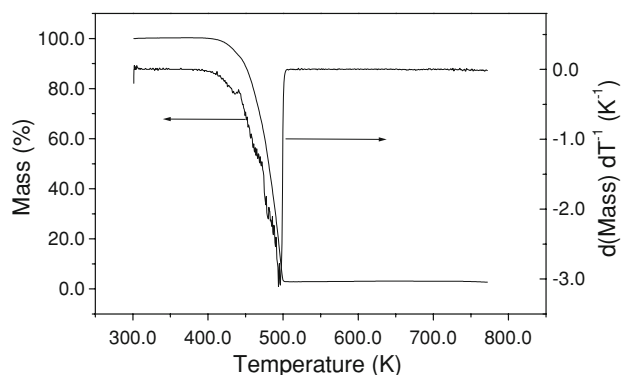
DSC curve (Fig. 3) shown three endothermic peaks in the temperature interval, except for adduct SbBr₃ · 4MPy indicating that the phase changes for these adducts occurred in one more step. First broad peak in the curves shown in Fig. 3 is belonging to the release of impurities as vaporization of traces of SbBr₃ (MP = 369 K) from the adducts. For curve in Fig. 3, the second peak was attributed the concomitant sublimation and decomposition processes of SbBr₃ · Py. Possible decomposition of the adducts was

indicated also by the change of the light color of the samples to dark above 453 K.

Data of three thermogravimetric curves obtained by linear heating using 5, 10 and 15 K min⁻¹ were processed by using Ozawa–Flynn–Wall analysis.

Table 3 Intervals of temperatures (T_1 , T_2 and T_3) and enthalpy from DSC data, and mass loss (ML) in the range of temperature (T) for SbBr₃ · L adducts where L is pyridine, 2-, 3- and 4-methylpyridines

SbBr ₃ · L	T_1 (K)	ΔH_1 (kJ mol ⁻¹)	T_2 (K)	T_3 (K)	ML (%)	T (K)
Py	387–417	2.30	417–460	460–503	97.3	400–503
2MPy	373–389	2.70	411–422	422–503	95.5	400–503
3MPy	381–395	0.74	412–425	425–546	95.5	400–503
4MPy	–	–	408–453	453–503	96.8	408–528

**Fig. 1** TG curves for adducts SbBr₃ · L where L is a Py b 2MPy c 3MPy and d 4MPy**Fig. 2** TG and DTG curves for SbBr₃ · Py

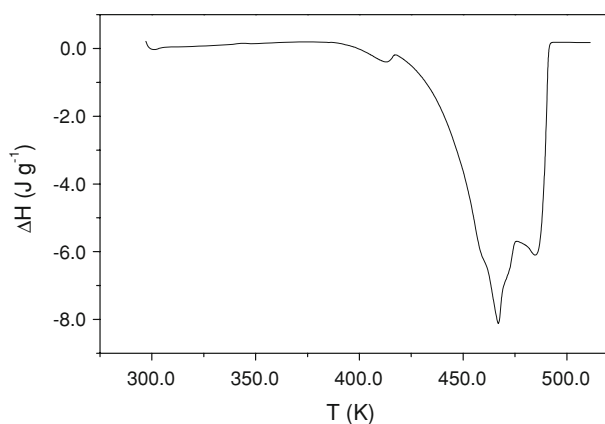


Fig. 3 DSC curve for $\text{SbBr}_3 \cdot \text{Py}$

$\text{SbBr}_3 \cdot \text{Py}$

The activation energy was constant for the conversion degree in the 10–30, 30–50 and 53–80% intervals, where E_a values were 150–147, 119–122 and $E_a = 134$ –136 kJ mol^{-1} , respectively. Kinetic parameters for the selected regions of conversion ($0.10 < \alpha < 0.30$) and ($0.53 < \alpha < 0.80$) were calculated by linear regression method of Coats–Redfern [17], considering only one step decomposition in each interval. The checking equations: R_2 , R_3 , F_n , D_2 , D_3 , A_2 and A_3 ; equation F_n for these intervals give as results: $E_a = 150.55 \text{ kJ mol}^{-1}$, $\log A = 16.0$ for $n = 0.67$; $E_a = 133.6 \text{ kJ mol}^{-1}$, $\log A = 13.9$ for $n = 0.55$ and $E_a = 142.33 \text{ kJ mol}^{-1}$, $\log A = 15.3$ for $n = 0.5$ (Table 4). These parameters are chosen on the basis of the approximate calculated values that are obtained by using mean model-free analysis method. The correlation coefficients are also approximately the same (0.9998, 0.9988 and 0.9996) at 5 K min^{-1} .

$\text{SbBr}_3 \cdot 2\text{MPy}$

The activation energy was constant for the conversion degree in the 7–50 and 75–95% intervals, where E_a values were 100–94 kJ and 90–85 kJ mol^{-1} , respectively. Kinetic parameters for the selected conversion ranges ($0.1 < \alpha < 0.5$) and

Table 4 Kinetic parameters derived from non-isothermal thermogravimetry according to Coats–Redfern for F_n and D_1 models in the interval of 10–30%

Adduct	E_a (kJ mol^{-1})	Log A (s^{-1})	Standard dev.	Model
$\text{SbBr}_3 \cdot \text{Py}$	150.6	16.0	$2.24 \cdot 10^{-4}$	F_n ($n = 0.67$)
$\text{SbBr}_3 \cdot 2\text{MPy}$	86.4	8.5	$1.27 \cdot 10^{-4}$	D_1 ($f(\alpha) = 1$)
$\text{SbBr}_3 \cdot 3\text{MPy}$	96.9	9.5	$0.98 \cdot 10^{-4}$	D_1 ($f(\alpha) = 1$)
$\text{SbBr}_3 \cdot 4\text{MPy}$	122.0	12.4	$2.04 \cdot 10^{-4}$	F_n ($n = 0.75$)

($0.75 < \alpha < 0.95$) were calculated by linear regression method of Coats–Redfern [17] also considering only one step decomposition in each interval. The checking equations: R_2 , R_3 , F_n , D_1 , D_2 , D_3 , A_2 and A_3 ; equation D_1 ($f(\alpha) = 1$) and F_n , with $n = 0.78$, for these intervals given: $E_a = 86.4 \text{ kJ mol}^{-1}$, $\log A = 8.5$; and $E_a = 80.1 \text{ kJ mol}^{-1}$, $\log A = 7.8$ (Table 4), respectively. These parameters are selected on the basis of the approximate calculated values that are obtained by using mean model-free method analysis. The correlation coefficients are also approximately the same (0.9999 and 0.9966) for rate of 5 K min^{-1} . A linear correlation ($r = 0.9999$) was obtained for the degree of conversion values determined by Ozawa–Flynn–Wall’s method and linear regression method of Coats–Redfern in the 7–50% interval.

$\text{SbBr}_3 \cdot 3\text{MPy}$

The activation energy was constant for the conversion degree in the 3–25 and 60–95% intervals, where E_a values were 101 and 83–86 kJ mol^{-1} , respectively. Kinetic parameters for the selected conversion region ($0.03 < \alpha < 0.25$) and ($0.60 < \alpha < 0.95$) were evaluated by Coats–Redfern linear regression method [17], considering only one step of decomposition in each interval. The checking equations: R_2 , R_3 , F_n , D_1 , D_2 , D_3 , A_2 and A_3 ; equation D_1 ($f(\alpha) = 1$) and F_n , with $n = 67$, for these intervals give as results: $E_a = 96.9 \text{ kJ mol}^{-1}$, $\log A = 9.5$; and $E_a = 83.85 \text{ kJ mol}^{-1}$, $\log A = 8.1$ (Table 4), respectively. These parameters are chosen on the basis of the approximate calculated values that are obtained by using mean model-free method analysis. The correlation coefficients are also approximately the same (0.9999, and 0.9996) for rate of 5 K min^{-1} .

$\text{SbBr}_3 \cdot 4\text{MPy}$

The activation energy was constant for the conversion degree in the 1–40 and 50–95% intervals, where E_a values were 159–154 and 96–84 kJ mol^{-1} , respectively. Kinetic parameters for the selected region of conversion ($0.08 < \alpha < 0.40$) and ($0.50 < \alpha < 0.95$) as for the other adducts also were calculated by Coats–Redfern method [17] take into account only one step decomposition in each interval. The checking equations: R_2 , R_3 , F_n , D_1 , D_2 , D_3 , A_2 and A_3 ; equations F_n and R_2 for these intervals give as results: $E_a = 122 \text{ kJ mol}^{-1}$, $\log A = 12.4$ for $n = 0.84$; and $E_a = 92.8 \text{ kJ mol}^{-1}$, $\log A = 8.8$ for R_2 equation (Table 4), respectively. The selection of these parameters based on the approximate calculated values that are obtained by using mean model-free method analysis. Correlation coefficients are also approximately the same (0.9998, and 0.9997) for rate of 5 K min^{-1} .

Conclusions

The pyridine 2-, 3- and 4-methylpyridine ligands reacted with antimony (III) tribromide forming $\text{SbBr}_3 \cdot \text{L}$ type adducts forming coordinating through nitrogen of aromatic ring. The kinetic studies obtained from TG data by using non-isothermal technique resulted the following kinetic parameters for E_a and $\log A$ (determined at 5 K min^{-1}) were $150.6 \text{ kJ mol}^{-1}$, 16.0 and $122.0 \text{ kJ mol}^{-1}$, 12.4 for $\text{SbBr}_3 \cdot \text{Py}$ and $\text{SbBr}_3 \cdot 4\text{MPy}$, respectively. For these adducts, the kinetic models are classified to F_n class with $n = 0.67$ and $n = 0.75$, respectively. For the two other adducts the kinetic parameters determined under the same conditions were 86.4 kJ mol^{-1} , 8.5 and 96.9 kJ mol^{-1} , 9.5 for $\text{SbBr}_3 \cdot 2\text{MPy}$ and $\text{SbBr}_3 \cdot 3\text{MPy}$, respectively. The best model was the phase boundary reaction, D1, for both adducts. While $\text{SbBr}_3 \cdot 2\text{MPy}$ and $\text{SbBr}_3 \cdot 3\text{MPy}$ showed the same thermal behavior, $\text{SbBr}_3 \cdot \text{Py}$ and $\text{SbBr}_3 \cdot 4\text{MPy}$ were slightly different from each other. The activation energy values suggested the following thermal stability order: $\text{SbBr}_3 \cdot \text{Py} \geq \text{SbBr}_3 \cdot 4\text{MPy}$ and $\text{SbBr}_3 \cdot 3\text{MPy} > \text{SbBr}_3 \cdot 2\text{MPy}$.

Acknowledgments The authors thank to CAPES and CNPq for financial support.

References

- Liptay G, Kenessey G, Bihatsi L, Wadsen T, Mink J. Pyridin type complexes of transition-metal-halides. *J Therm Anal.* 1992;38: 899–905.
- Liptay G, Kenessey G, Mink J. Pyridine type complexes of transition-metal-halides II: Preparation, characterization and thermal analysis studies of cobalt(II)-bromides and iodides with 2-,3-,4-methylpyridines. *Thermochim Acta.* 1993;214:71–83.
- Mautner FA, Goher MAS. Synthesis, spectroscopic and crystal structure study of di- μ (1,1)-azido- μ (*O,O*)-nitrate(*O*-nitrate)tetrakis(3-picoline) aquadecopper(II) and catena-di- μ (1,3)-azido-[di- μ (1,1)-azido-bis(4-picoline)dicopper(II)][$\text{Cu}_2(\text{N}_3)_2(\text{NO}_3)_2$ (3-picoline) $_4(\text{H}_2\text{O})$] and $\text{Cu}(4\text{-picoline})(\text{N}_3)_2$. *Polyhedron.* 1993;12: 2823–9.
- Sultana N, Tabassum H, Arayne MS. Synthesis and characterization of Cu(I) complexes of triphenylphosphine and 2-methylpyridine. *Indian J Chem A.* 1994;33:63–4.
- Mautner FA, Goher MAS. Spectral and X-ray structure determination of two polymeric complexes of copper(II) azide with 3-picoline and 2-bromopyridine: $\text{Cu}(3\text{-picoline})_2(\text{N}_3)_2$ and $\text{Cu}(2\text{-bromopyridine})(\text{N}_3)_2$. *Polyhedron.* 1992;11:2537–42.
- Kiran S, Ravi K, Prem R, Goswami AK. Synthesis and characterization of bis(pentafluorophenyl)antimony(V) cations, $[(\text{C}_6\text{F}_5)_2\text{SbL}_3]^{3+}$. *J Fluorine Chem.* 2003;122:229–32.
- Srinivas N, Kishan MR, Kulkarni SJ, Raghavan KV. Ammoxidation of picolines over modified silicoaluminophosphate molecular sieves. *Microporous Mesoporous Mater.* 2000;39:125–34.
- Das SC. Evaluation of some organic additives for zinc electro-winning from sulphate solutions. *Trans Indian Inst Met.* 1999;49: 781–8.
- Das SC, Singh P, Hefter GT. Effects of 2-picoline on zinc electro-winning from acidic sulfate electrolyte. *J Appl Electrochem.* 1996;26:1245–52.
- Dunstan PO, Airoidi C. Adducts of arsenic trihalides with heterocyclic amines. *J Chem Eng Data.* 1988;33:93–8.
- Ptaszynski B. The thermal-decomposition of complex salts of bismuth(III) bromide with hydrobromides of aromatic-amines. *Thermochim Acta.* 1994;232:137–44.
- Pontes FML, Oliveira SF, Espínola JGP, Fonseca MG, Arakaki LNH. Picoline as ligand with antimony trichloride and triiodide adducts. *J Therm Anal Calorim.* 2004;75:975–88.
- Ozawa T. A new method of analyzing thermogravimetric data. *Bull Chem Soc Jpn.* 1965;38:1881.
- Flynn J, Wall LA. A quick direct method for determination of activation energy from thermogravimetric data. *Polym Lett.* 1966;4:232–7.
- Brown ME, Dollimore D, Galwey AK. *Comprehensive chemical kinetics*, vol. 22. Amsterdam: Elsevier; 1980.
- Ribeiro CA, de Souza WR, Crespi MS, Gomes Neto JA. Non-isothermal kinetic of oxidation of tungsten carbide. *J Therm Anal Calorim.* 2007;90:801–5.
- Logvinenko V. Model-free approach in the study of decomposition kinetics for cluster compounds and coordination compounds. *J Therm Anal Calorim.* 2008;93:805–9.
- Vadim M, Serge B. Modulated thermogravimetry in analysis of decomposition kinetics. *Chem Eng Sci.* 2005;60:747–66.
- Cotas AW, Redfern JP. Kinetics parameters from thermogravimetric data. *Nature.* 1964;201:68–9.
- Green JHS, Kynaston W, Paisley HM. Vibrational spectra of monosubstituted pyridines. *Spectrochim Acta.* 1963;19:549–64.
- Lamba OP, Parihar JS, Jaint YS. Laser-excited Raman and infrared-spectra of alpha-picolines, beta-picolines and gamma-picolines. *Indian J Pure Appl Phys.* 1983;21:236–42.